Effect of antimony on the eutectic reaction of heavy section spheroidal graphite castings

P. Larrañaga[1], I. Asenjo[1], J. Sertucha[1], R. Suárez[1], I. Ferrer[2] and J. Lacaze*[3]

There is a strong demand for heavy section castings made of spheroidal graphite with a fully ferritic matrix, e.g. for manufacturing hubs for windmills. Such castings with slow solidification process are prone to graphite degeneration that leads to a dramatic decrease of the mechanical properties of the cast parts. Chunky graphite is certainly the most difficult case of graphite degeneracy, though it has long been known that the limited and controlled addition of antimony may help eliminate it. The drawback of this remedy is that too large Sb additions lead to other forms of degenerate graphite, and also that antimony is a pearlite promoter. As part of an investigation aimed at mastering low level additions to cast iron melts before casting, solidification of large blocks with or without Sb added was followed by thermal analysis. Comparison of the cooling curves and of the microstructures of these different castings gives suggestions to understand the controlling nucleation and growth mechanisms for chunky graphite cells.

Keywords: Nodular cast iron, Spheroidal growth, Cooling curve, Chunky graphite, Antimony

Introduction

In commercial cast irons, chunky graphite (CHG) forms in the central area (thermal centre) of large castings, though it may appear also in thin sections.[1] Macroscopic observation shows a sharp transition as illustrated in Fig. 1*a* that could not be related to any significant macrosegregation.[2–4] Figure 1b illustrates the microstructure as most generally observed by optical microscopy in the areas affected by CHG. It is seen dendrite-like ex-austenite with large nodules embedded in, more or less rounded cells of CHG and the usual spheroidal graphite (SG) microstructure in the remaining area. In these latter areas, graphite nodules are much smaller and numerous than those in the dendrite-like areas, they will be denoted as secondary nodules while the large nodules will be denoted as primary.

CHG cells have been since long recognized to consist of interconnected and branched graphite,[5,6] as illustrated in Fig. 2*a*. They should develop through a coupled growth process between graphite and austenite that has been suggested to be slightly looser than for lamellar cells.[7] Moreover, it is now clearly established that the growth process of CHG graphite is totally different to the growth of lamellar graphite, and instead much similar to growth of SG.[5,6,8] It may be viewed as growth of irregular crystallites along the c direction, graphite layers piling up as observed in SG.[5,8] As a matter of fact, many authors noted that the graphite particles get coarser and rounded at the periphery of CHG cells, approaching SG growth. This is illustrated in Fig. 2*b* that was obtained from the same sample than for Fig. 2*a*.

Although a great number of studies has been devoted to the description of CHG formation, a clear understanding of its appearance and a safe mastering of metal preparation to avoid it are not yet available. In this study, the solidification behaviours of large blocks with or without addition of Sb are compared by means of the cooling curves recorded during casting and by means of microstructure observation. The results are discussed with particular emphasis put on the effect of Sb while the role of post-inoculation has been described previously.[9]

Experimental details

Cubic blocks with size L=300 mm were cast in sand moulds according to the methodology described previously,[9] they have a thermal modulus about 5 cm. Each casting consisted of two to four blocks connected to the same gating system. Post-inoculation and addition of Sb were performed as required by fixing appropriate materials with a foundry adhesive close to the selected block entrance within the gating system. Post-inoculation was made with a commercial inoculant (70–78 Si, 3·2–4·5 Al, 0·3–1·5 Ca and ~0·5 RE, wt-%). When appropriate, an addition of Sb was performed with 99·99 % pure element, to reach a level of 0·004 to 0·010 % of the block weight. Table 1 lists the composition of the four cast melts as measured on medals taken before pouring in the mould, apart from the Sb content which was measured on the blocks using an ICP–MS technique. All other elements than those listed were at

[1]Engineering and Foundry Department, AZTERLAN, Aliendalde auzunea 6, E-48200 Durango (Bizkaia), Spain
[2]TS Fundiciones, S.A. Pol. Sansinenea Erreka, E-20749 Arroa-Zestoa (Gipuzkoa), Spain
[3]CIRIMAT, UMR 5085 CNRS/UPS/INPT, ENSIACET, 31077 Toulouse cedex 4, France

*Corresponding author, email Jacques.lacaze@ensiacet.fr

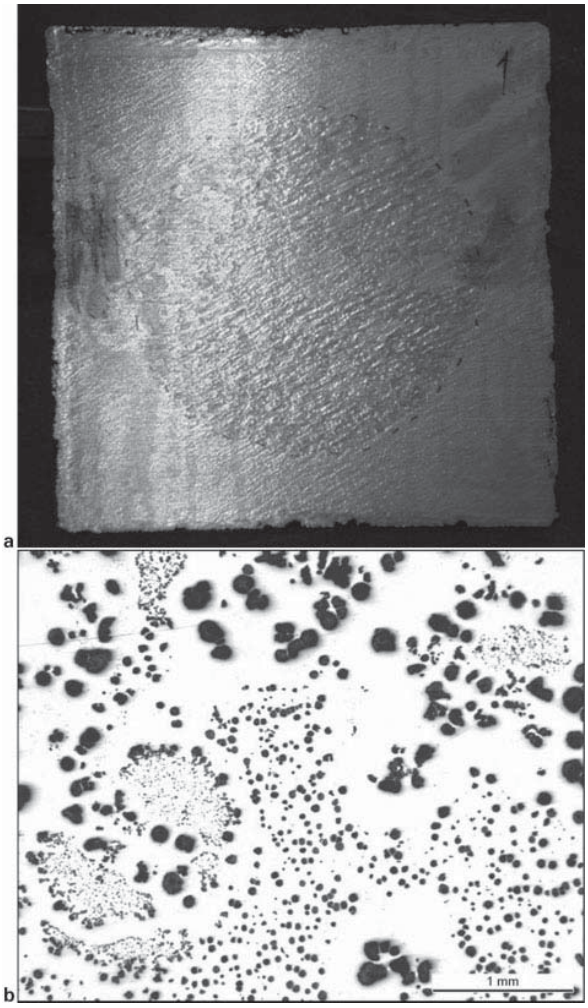

1 *a* Central section of a cast block with the zone affected by CHG appearing with darker contrast; *b* Optical micrograph of a heavy section SG cast iron part showing dendrite-like ex-austenite with large nodules embedded in, cells of CHG and areas of usual SG microstructure

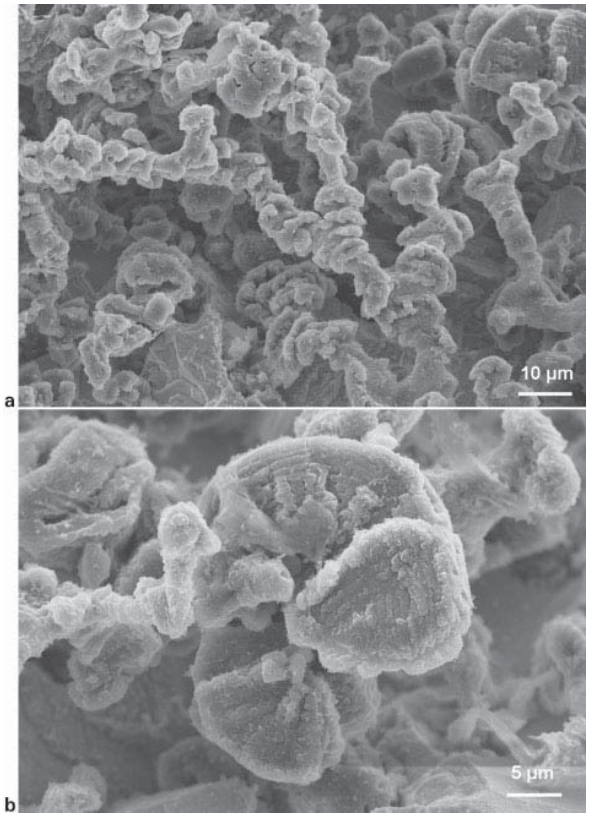

2 *a* Interconnected strings of graphite crystallites as observed in SEM on a deeply etched sample; *b* Termination of a graphite string with an incomplete graphite nodule

very low but reproducible levels.[9] The differences in cerium content that appear in Table 1 are due to the use of various FeSiMg alloys for the nodularizing treatment of the melts. Besides, 0·034% of Ce-rich misch-metal was added to the melt during the Mg-treatment performed for the M5-13 trial. The stable eutectic temperature of these alloys is predicted to vary from 1162·7 to 1163·3°C depending on the composition.[10] In the following, the various blocks will be labelled as M5–X–Y, where M5 is for the modulus, X indicates the trial number (12, 13, 16 or 18), Y stands for no post-inoculation (N), post-inoculation (I), post-inoculation and addition of Sb (ISb). In the case of M5-16 trial, two levels of Sb were added that are additionally labelled with a and b.

All cast blocks were equipped with a single K-type thermocouple positioned at the geometrical centre for recording the cooling curves during solidification and cooling. An additional thermocouple was located at L/6 from the outer surface of the two blocks cast during trial

Table 1 Code of the castings, use of post-inoculation (I for inoculated) or not (N for no inoculation), composition of the melt in carbon, silicon, cerium and antimony (in wt-%), carbon equivalent (calculated as $C_{eq}=w_C+0{\cdot}28w_{Si}$[10]), nodules counts N (mm^{-2}), volume fraction of the block V_V (%) and area fractions A (%) affected by CHG (see text for details)

Trial	Block	w_C	w_{Si}	w_{Ce}	w_{Sb}	C_{eq}	V_V	A_A	N_{block}	A_{PG}	N_{PG}	A_{SG}	N_{SG}
M5-12	ISb	3·68	2·20	0·0123	0·0095	4·30	0·5	1·0	90	44	15	55	150
	I				<0·0002		18·0	47·0	83	32	48	21	137
M5-13	N	3·73	2·08	0·0162	<0·0002	4·31	0·1	50·0	25	19	9	31	35
	I				<0·0002		15·0	14·0	63	32	41	54	76
	ISb				0·0108		2·0	7·0	94	25	64	68	105
M5-16	ISb-a	3·72	2·08	0·0100	0·0043	4·30	7·0	10·0	81	20	67	70	85
	ISb-b				0·0071		4·0	20·0	89	31	84	49	92
	I				<0·0002		22·0	5·0	110	21	110	74	110
	N				<0·0002		0·5	50·0	39	16	33	34	42
M5-18	ISb	3·71	2·07	0·0028	0·0095	4·29	0·0	0·0	70	16	49	84	74
	I				<0·0002		24·0	6·0	88	24	9	70	115

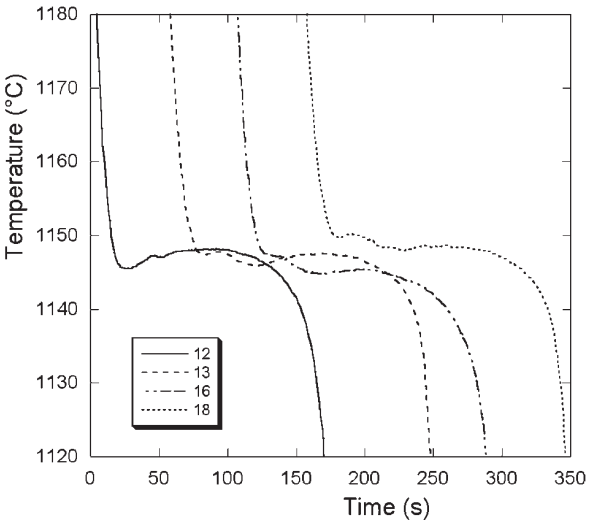

3 Cooling curves recorded on the TA cups for melts with post-inoculation

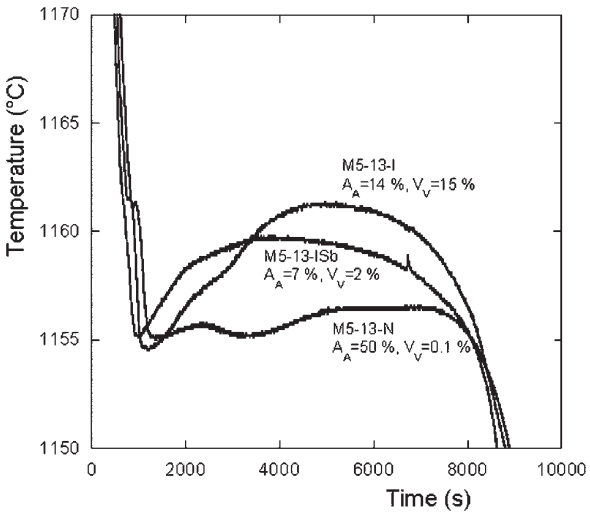

4 Comparison of the cooling curves obtained at the thermal centre of the three blocks of trial M5-13 with A_A and V_V values indicated

M5-18. Because of a different positioning of the blocks in this latter trial, the effective thermal modulus was in fact higher than for the other castings at about 6 cm. Also, just before casting the blocks, some metal was poured in two standard TA cups, one of them containing powder of inoculant so as to reach the same level than the one for the blocks.

After casting, the blocks were sectioned and the volume fraction V_V of the blocks affected by CHG was measured from images such as the one in Fig. 1*a*.[9] Metallographic sections were then prepared from samples taken at the centre of the casting, on which series of micrographs such as the one in Fig. 1*b* were made for measuring the local area fraction A_A of CHG.[9] On similar series of micrographs, the areas A_{PG} and A_{SG} with respectively primary and secondary graphite nodules as well as the corresponding nodule densities N_{PG} and N_{SG} were estimated. All these values are listed in Table 1, as well as the average nodule count N_{block} which is given as: $(100-A_A)\times N_{block}=A_{PG}\times N_{PG}+A_{SG}\times N_{SG}$.

Results

Thermal analysis with standard TA cups are shown in Fig. 3 for inoculated alloys which show that solidification proceeds in two steps, much like the description given by Chaudhari *et al.*[11] for near eutectic alloys, with an initial eutectic reaction and a more lengthy eutectic plateau. These curves confirm also that all four melts have similar solidification features in relation to their nearly identical carbon equivalent C_{eq} (see Table 1). This was the case also for the curves recorded with non-inoculated alloys though, as expected, it was noted that post-inoculation increases significantly the eutectic plateau temperature.

None of the TA cups did show any CHG, so that the cooling curves recorded on the blocks were first analysed with the aim of looking for any difference with the TA cups records and for any relationship between their characteristics and the amount of CHG as measured either with A_A or V_V. In that respect, attention should be put on the recalescence as it has been reported that it increases with CHG formation.[1,4] Figure 4 provides a comparison of the cooling curves recorded on the blocks M5-13-N, M5-13-I and M5-13-ISb. The eutectic solidification proceeds in two steps as for the TA cups, though the two arrests have somehow merged in the case of the melt treated with Sb. There is also a pre-eutectic reaction that is apparent for all the three curves. The effect of post-inoculation is clearly evidenced with a recalescence rate for the first eutectic reaction being much higher after this treatment (M5-13-I and M5-13-ISb) than without it (M5-13-N).

The corresponding values of A_A and V_V have been also reported along the curves in Fig. 4. In the case of the non post-inoculated melt, it is seen that the high value of A_A is not related to a large recalescence, thus indicating that the cooling curve characteristics do not relate to local microstructure evolution. The same was observed with the cooling curve recorded on the M5-16-N block. On the contrary, there is clearly a higher recalescence during the second eutectic reaction of the M5-13-I when compared to the Sb-treated M5-13-ISb block. As a matter of fact, this increased rate could be observed for all castings that were inoculated but not treated with Sb. Owing to the higher nodule counts of both primary and secondary graphite in the case of the Sb treated melt, as well as to the lower amount of CHG, the higher recalescence observed for the melt without Sb could well be related to CHG formation.

The above conclusions were confirmed by the analysis of the two cooling curves recorded on each of the blocks of trial M5-18. The comparison of the records at the distance L/6 from the surface of the blocks with and without Sb added is made in Fig. 5. The two curves are superimposed until about one third of the solidification time, and then a strong recalescence appears in the case of the untreated block. As the microstructure of these castings differ by the fact that Sb suppresses totally CHG while V_V was found equal to 24% in the non-treated block, it seems evident to associate the increase in the recalescence rate to the growth of CHG. The curves recorded at the centre of the blocks showed exactly the same features, at exactly the same time, meaning that the temperature of the material is

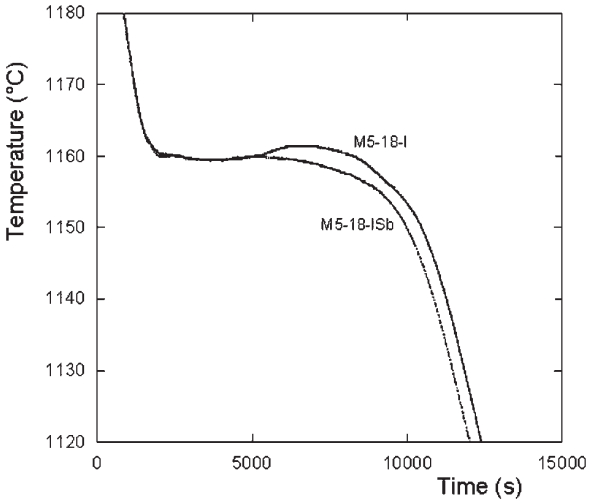

5 Comparison of the cooling curves recorded during trial M5-18 at L/6 on the blocks with and without Sb added

homogeneous after an initial transient. Thus, the melt cools down and then starts to solidify in a nearly uniform way in the whole block, and temperature gradients take place only after a significant fraction of the material has solidified. The cooling curves appear to be representative of the solidification at the scale of the blocks, thus explaining why no correlation could be found between A_A and V_V values and the eutectic plateau temperature. This also agrees with the conclusion by Prinz *et al.*[4] who reported that recalescence is limited when CHG is concentrated in the centre of the castings and maximum when the whole section is affected.

Discussion and conclusion

The shape of the pre-eutectic reaction observed in the cooling curves of Fig. 4 is similar to what could be expected for primary precipitation of graphite. This appears in agreement with the fact that in most cases blocks showed a microstructure as illustrated in Fig. 1*b* with large nodules embedded in dendrite-like ex-austenite. The first eutectic reaction thus appears related to the coupled growth of these primary nodules with austenite, and it has been seen its kinetics is enhanced with higher nodule count. It was however also observed that the undercooling between the primary arrest and the start of the eutectic reaction is correlated with the amount of cerium, in agreement with previous observations,[12] and not with nodule count. In line with the schematic by Zhou *et al.*,[7] it is concluded from the above results that CHG cells nucleate during the initial eutectic reaction, once austenite dendrites with primary graphite nodules embedded within it have started to develop. Their growth leads to a sharp slope change on the eutectic plateau, corresponding to an increased recalescence rate.

Owing to the very small composition differences between the alloys presently studied, it was noted that the undercooling of the melt at the start of the eutectic reaction, which should relate to its carbon supersaturation, greatly varies from one casting to another without a direct relation to the amount of CHG formed. This suggests that the proposal by Gagne and Argo[2] that CHG increases with constitutional supercooling of the melt should be further substantiated. One line for future work emerged by the observation that oxides or compounds found in CHG areas differ from those observed in unaffected zones.[3] As a matter of fact, the lengthy cooling and solidification time of heavy section SG irons may allow for significant changes in the amount of active elements dissolved in the melt. Accordingly, one may have to consider nucleation and growth of oxides or other compounds of Mg, Ce or any other additive or impurity, for a proper understanding of the formation of CHG.

Acknowledgements

This paper is based on work supported by the Industry Department of the Spanish Government (PROFIT FIT-030000-2007-94). Thanks are due to Yannick Thébaut for SEM images and to Luiz Eleno for translating papers written in German.

References

1. R. Källbom, K. Hamberg, M. Wessén and L. E. Björkegren: *Mater. Sci. Eng.*, 2005, **A413–414**, 346–351.
2. M. Gagné and D. Argo: Proc. Int. Conf. on 'Advanced casting technology', Easwaren J. ed., 231–256; 1987, Metals Park, OH, ASM.
3. R. Källbom, K. Hamberg and L. E. Björkegren: Proc. 67th World Foundry Congress, 2006, Harrogate, UK, paper 184.
4. B. Prinz, K. J. Reifferscheid, T. Schulze, R. Döpp and E. Schürmann: *Giessereiforschung*, 1991, **43**, 107–115.
5. P. C. Liu, C. L. Li, D. H. Wu and C. R. Loper: *Trans. AFS*, 1983, **91**, 119–126.
6. T. C. Xi, J. Fargues, M. Hecht and J.-C. Margerie: *MRS. Symp. Proc.*, 1985, **34**, 67–76.
7. Jiang Zhou, W. Schmitz and S. Engler: *Giessereiforschung*, 1987, **39**, 55–70.
8. H. Itofuji and H. Uchikawa: *AFS Trans.*, 1990, **98**, 429–448.
9. I. Asenjo, P. Larrañaga, J. Sertucha, R. Suárez, I. Ferrer, J. M. Gómez and J. Lacaze: Int. J. Cast Met. Res., 2007, **20**, 319–324.
10. M. Castro, M. Herrera, M. M. Cisneros, G. Lesoult and J. Lacaze: *Int. J. Cast Met. Res.*, 1999, **11**, 369–374.
11. M. D. Chaudhari, R. W. Heine and C. R. Loper: *AFS Trans.*, 1974, **82**, 379–386.
12. P. K. Basutkar and C. R. Loper: *AFS Trans.*, 1971, **79**, 176–185.